

# REPORT DOCUMENTATION PAGE

*Form Approved*  
*OMB No. 0704-0188*

Public reporting burden for this collection of information is estimated to average 1 hour per response, including the time for reviewing instructions, searching existing data sources, gathering and maintaining the data needed, and completing and reviewing this collection of information. Send comments regarding this burden estimate or any other aspect of this collection of information, including suggestions for reducing this burden to Department of Defense, Washington Headquarters Services, Directorate for Information Operations and Reports (0704-0188), 1215 Jefferson Davis Highway, Suite 1204, Arlington, VA 22202-4302. Respondents should be aware that notwithstanding any other provision of law, no person shall be subject to any penalty for failing to comply with a collection of information if it does not display a currently valid OMB control number. **PLEASE DO NOT RETURN YOUR FORM TO THE ABOVE ADDRESS.**

<b>1. REPORT DATE (DD-MM-YYYY)</b> 14-10-2009		<b>2. REPORT TYPE</b> Journal Article		<b>3. DATES COVERED (From - To)</b>	
<b>4. TITLE AND SUBTITLE</b>  <b>Impact of Vane Size and Separation on Radiometric Forces for Microactuation (Preprint)</b>				<b>5a. CONTRACT NUMBER</b>	
				<b>5b. GRANT NUMBER</b>	
				<b>5c. PROGRAM ELEMENT NUMBER</b>	
<b>6. AUTHOR(S)</b> Natalia Gimelshein and Sergey Gimelshein (ERC), Andrew Ketsdever (AFRL/RZSP), Nathaniel Selden (USC)				<b>5d. PROJECT NUMBER</b>	
				<b>5e. TASK NUMBER</b>	
				<b>5f. WORK UNIT NUMBER</b> 50260542	
<b>7. PERFORMING ORGANIZATION NAME(S) AND ADDRESS(ES)</b>  Air Force Research Laboratory (AFMC) AFRL/RZSA 10 E. Saturn Blvd. Edwards AFB CA 93524-7680				<b>8. PERFORMING ORGANIZATION REPORT NUMBER</b>  AFRL-RZ-ED-JA-2009-368	
<b>9. SPONSORING / MONITORING AGENCY NAME(S) AND ADDRESS(ES)</b>  Air Force Research Laboratory (AFMC) AFRL/RZS 5 Pollux Drive Edwards AFB CA 93524-7048				<b>10. SPONSOR/MONITOR'S ACRONYM(S)</b>	
				<b>11. SPONSOR/MONITOR'S NUMBER(S)</b> AFRL-RZ-ED-JA-2009-368	
<b>12. DISTRIBUTION / AVAILABILITY STATEMENT</b>  Approved for public release; distribution unlimited (PA #09471).					
<b>13. SUPPLEMENTARY NOTES</b> For the Microfluidics and Nanofluidics Journal					
<b>14. ABSTRACT</b> A kinetic approach is used to study the feasibility of increasing the efficiency of microactuators that use radiometric force through etching holes in a single radiometer vane. It has been shown that a radiometer that consists of small vanes is capable of producing at least an order of magnitude larger force than a single vane radiometer that takes up the same area. The optimum gap between the vanes is found to be slightly smaller than the vane size, with the optimum Knudsen number of about 0.05 based on the vane height. Several competing processes have been suggested for the actuation of micromechanical devices. Electrostatic micro-actuators have been suggested <sup>1, 2</sup> where a potential difference between two sets of combs produces a force generated by the associated electric field. Generally, electrostatic micro-actuators are linear drive devices and are not well suited for rotational operation. Piezoelectric devices <sup>3</sup> have been considered where an electric field applied to a material causes mechanical deformation in the material. The piezoelectric effect typically produces very small material deflections; however, they can have a very fast actuation frequency from the kHz up to the MHz range. Electrically conducting polymers <sup>4</sup> can be used to change the volume of a material to provide more actuation distance than a typical piezoelectric material with lower applied voltages.					
<b>15. SUBJECT TERMS</b>					
<b>16. SECURITY CLASSIFICATION OF:</b>			<b>17. LIMITATION OF ABSTRACT</b>	<b>18. NUMBER OF PAGES</b>	<b>19a. NAME OF RESPONSIBLE PERSON</b>
<b>a. REPORT</b>	<b>b. ABSTRACT</b>	<b>c. THIS PAGE</b>			Marcus Young
Unclassified	Unclassified	Unclassified	SAR	19	<b>19b. TELEPHONE NUMBER</b> (include area code) N/A

# Impact of Vane Size and Separation on Radiometric Forces for Microactuation

Natalia Gimelshein and Sergey Gimelshein<sup>1</sup>

*ERC, Inc., Edwards AFB, CA 93524*

Andrew Ketsdever

*Propulsion Directorate, Edwards AFB, CA 93524*

Nathaniel Selden

*University of Southern California, Los Angeles, CA 90089*

A kinetic approach is used to study the feasibility of increasing the efficiency of microactuators that use radiometric force through etching holes in a single radiometer vane. It has been shown that a radiometer that consists of small vanes is capable of producing at least an order of magnitude larger force than a single vane radiometer that takes up the same area. The optimum gap between the vanes is found to be slightly smaller than the vane size, with the optimum Knudsen number of about 0.05 based on the vane height.

**Keywords:** Microactuation, radiometric force, multiple vanes, ES BGK

---

<sup>1</sup>Corresponding author. Address: 854B Downey Way, RRB-230, Los Angeles, CA 90089.

Tel.: +1-213-740-9211. Fax: +1-213-821-5819. Email: gimelshe@usc.edu

## I. Introduction

Several competing processes have been suggested for the actuation of micromechanical devices. Electrostatic micro-actuators have been suggested<sup>1,2</sup> where a potential difference between two sets of combs produces a force generated by the associated electric field. Generally, electrostatic micro-actuators are linear drive devices and are not well suited for rotational operation. Piezoelectric devices<sup>3</sup> have been considered where an electric field applied to a material causes mechanical deformation in the material. The piezoelectric effect typically produces very small material deflections; however, they can have a very fast actuation frequency from the kHz up to the MHz range. Electrically conducting polymers<sup>4</sup> can be used to change the volume of a material to provide more actuation distance than a typical piezoelectric material with lower applied voltages. The actuation range of a micro-actuator based on an electrically conducting polymer is still relatively limited (10 $\mu$ m maximum). Thermo-pneumatic<sup>5</sup> and other gas dynamic actuators<sup>6</sup> offer the potential for relatively large forces (1000 times greater than electrostatic forces) per unit volume and large actuation distances. Radiometric forces have also been proposed in the literature.<sup>7-9</sup> Micro-actuators based on radiometric forces offer several distinct advantages over other proposed concepts including simplicity, scalability, and an unlimited actuation range. Although radiometric forces have been suggested as a possible means for the actuation of micromechanical devices for more than a decade,<sup>7</sup> a radiometric-based actuator has yet to be realized.

Radiometric flows and their associated forces are typically thought of only in the low pressure, rarefied gas regime where their effects can be large compared to other forces. The level of gas rarefaction is given by the non-dimensional Knudsen number

$$Kn = \lambda/L$$

where  $\lambda$  is the gas mean free path and  $L$  is a characteristic dimension in the flow. The rarefied gas regime is generally considered the regime where the Knudsen number is relatively large compared to the continuum flow regime. The rarefied regime can be characterized as having Knudsen numbers larger than 0.01. Traditionally, this has meant the regime where the mean free path is large corresponding to low pressure applications. However, the advent of micro-fabrication and microfluidics has brought about the concept of rarefied flow at atmospheric (or slightly above) pressures where the characteristic size of the device is very small. For

example if the characteristic dimension of a device,  $L$ , is  $1\ \mu\text{m}$ , the Knudsen number is 0.1 for a pressure of one atmosphere. Therefore in a micro-device, radiometric flows can be a dominant force even at relatively high pressure. From the application standpoint, there is the critical benefit of not requiring a vacuum to be created or maintained for this device as a micro-actuator.

The radiometric force is produced by a temperature gradient between nearby surfaces in a rarefied flow (high Knudsen number). An excellent review of the history associated with radiometric flows can be found in Ref.<sup>10</sup> Force is produced in a radiometer by the temperature gradient in two ways. First, a pressure difference between the gas on the high temperature side and the low temperature side produces a net force. Since the pressure near the high temperature surface is larger than that on the low temperature surface, this pressure force acts from hot to cold, henceforth called the area force. Second, thermal creep<sup>11</sup> in the form of a shear force acts along the edge of the radiometer in the direction from cold to hot, henceforth called the edge force.

Recently, new studies<sup>10,12,13</sup> have shed light on the fundamental understanding of radiometric flows and their engineering applications, allowing for significant improvement in the theoretical design of radiometric micro-actuators. The knowledge gained in these previous studies has been combined into the design of a notional device that maximizes the radiometric force produced in a given volume. Any attempt to optimize the radiometer design for force production requires a fundamental understanding of the relative influence of the bulk radiometer area versus the radiometer edge. Recent results indicate that these effects are of the same order of magnitude in the Knudsen number regime where the force is maximized (transitional regime,  $\text{Kn } 0.05$ ). Therefore, a device that maximized the force produced per unit volume (or mass) will be an optimized combination of area and edge geometry. This paper describes a notional radiometric-based micro-actuator that produces a maximum force at typical Knudsen numbers for micro-scale actuators operating at or slightly above atmospheric pressure.

Although the major application of the effect described in this work is for micro-devices, applications in the low pressure regime (same equivalent Knudsen number) can also be envisioned. For example, radiometric forces could be applicable to propulsion systems for vehicles traveling at high altitudes (i.e. near-space).<sup>14</sup> In these applications, solar energy could be used to generate temperature differences between two surfaces separated over a distance. The radiometric force could be used in a propulsion system as a means of

maintaining a near-space vehicle's position above the Earth while compensating for disturbing forces such as wind drag.

## II. Numerical approach and flow conditions

The selection of the numerical method for modeling microscale gas flows is dictated by the relative importance of physical phenomena inherent in these flows, such as velocity slip, temperature jump, thermal creep, and viscous heating. The small physical scale usually implies large surface-to-volume ratios, thus emphasizing the influence of gas-surface interactions. In addition, the gas mean free path is often comparable to the characteristic dimensions of the flow, causing the velocity distribution function to deviate from local equilibrium. All this results in inapplicability of shear stress and heat flux assumptions used in the Navier-Stokes equations and many analytic approaches, and leaves the computational methods of the kinetic gas theory as the only alternative.

The principal equation of the kinetic theory, the Boltzmann equation, which tracks the evolution of the velocity distribution function impacted by the molecular motion and collisions, is too complex and its analytical solution is not possible for any realistic flow scenario. Numerical approaches to the Boltzmann equation, such as the direct numerical integration or the direct simulation Monte Carlo method, are time-accurate methods and as such are extremely time consuming for low speed microscale flows, where the time to reach steady state measures in seconds. A plausible numerical alternative is a deterministic solution of one of the simplified forms of the Boltzmann equation, known as model kinetic equations. Two of the better known model kinetic equations, the Bhatnagar-Gross-Krook (BGK)<sup>15</sup> and the ellipsoidal statistical (ES)<sup>16</sup> kinetic models, use a non-linear relaxation term instead of the full Boltzmann collision integral. In spite of the simpler collision term, both models possess the same collision invariants as the Boltzmann equation. The existence of numerically efficient implicit integration schemes for these equations<sup>17</sup> allows for accurate numerical modeling of microflows at a reasonable computational cost.

In this work, a finite volume solver SMOKE<sup>18</sup> has been used to deterministically solve the ES model kinetic equation. SMOKE is a parallel code based on conservative numerical schemes developed by.<sup>17</sup> The code has both two-dimensional and axisymmetric capabilities. In the computations presented below, only the two-dimensional capability is used. A second order spatial discretization was utilized along with implicit

time integration. Fully diffuse reflection with complete energy accommodation was applied at the radiometer vane and chamber walls. A symmetry plane was set at the lower boundary.

In what follows, all spatial dimensions are normalized by the height  $D$  of the radiometer vane in the single vane setup,  $D = 1.1$  mm. Two chamber sizes were considered in order to analyze the impact of the proximity of chamber walls,  $0.45D \times 1.5D$  and  $1.1D \times 1.7D$ . Both single vane and multiple vane configurations were considered, and in all cases, the total area occupied by the radiometric device was  $D$ . The thickness of radiometer vanes was kept at  $0.01D$ . The gas pressure was ranging from about 20 Pa to 6,000 Pa, and Knudsen number varies over 10 (nearly free molecule flow) to less than 0.01 (near continuum flow). This allowed us to capture the maximum in the radiometric force, typically observed at a Knudsen of about 0.1.<sup>10,12</sup> Here and below, Knudsen numbers are calculated as the ratio of the the gas mean free path in the free stream (undisturbed flow far from the radiometer) to the height of the vane (either the single vane or one of the multiple vanes in multi-vane configurations) . The gas mean free path is evaluated with a VHS/VSS model expression given by Eqn. (4.65) in.<sup>19</sup> Pure argon was chosen as the carrier gas in this work.

The grid convergence was achieved by increasing the number of spatial nodes and points in the velocity space. The latter one was (18,18,12) for the results presented below, and the number of spatial cells varied from 5,000 to 10,000 depending on the chamber size. The temporal convergence was also controlled, and the total error in the force calculations was estimated to be less than one percent in all cases. In all computations, the temperature of the hot and cold sides of the vanes was 450 K and 410 K, respectively, and the chamber wall surface temperature was assumed to be 300 K. It is important to note that the relatively large temperature difference was chosen to emphasize the effect of the temperature gradient and make it easier for accurate numerical analysis. The qualitative results presented below will not change for a different temperature gradient, or different radiometer size, provided the Knudsen numbers are still the same. This implies that the results will not change if for example a larger radiometer of 1.1 cm is considered in a ten times more rarefied carrier gas.

### III. Optimum separation between the vanes

The main objective of this work is to analyze the feasibility of increasing the radiometric force through etching holes in the radiometric vane. This goal implies that the total area occupied by the radiometer is

fixed, but the number of small vanes (smaller parts of the original large radiometer vane) separated by gaps and the separation distance between them may vary to satisfy the maximum radiometric force requirement. The optimization in terms of the vane to gap height ratio generally implies finding either the separation between the vanes that results in maximum total force produced by the radiometer, or the separation that is characterized by maximum force per vane (or, in other words, force per radiometer mass). While both optimizations are important, the second one is considered in more detail in this work.

The first set of computations was therefore aimed at finding the optimum force-per-mass separation distance between the small vanes relative to their height. In these computations, the size of the small vanes was fixed at  $0.09D$ , and the separation between them ranged from  $0.92D$  to about  $0.035D$ . Comparison of the translational temperature fields and the streamlines is presented for two-vane and seven-vane configurations in Fig. 1. The flowfields represent only half of the entire flow, since the lower boundary is the symmetry plane. The other three boundaries represent the chamber walls. Hereafter, the left side of the radiometer is hot, and the cold side is hot.

For the two-vane configuration, the interference between the vanes is minimal. Near the symmetry axis, the gas temperature is a few degrees higher than it could be expected in the absence of the second vane. Near the vane, however, the isolines are symmetric relative to the center of the vane, which indicates that a relatively small effect of the lower vane and the top wall of the chamber. The impact of the cold top wall of the chamber is seen in the streamlines near at the cold side, that are asymmetric. There is only one vortex observed at that side as compared to two vortices for a single vane configuration.<sup>13</sup> The interference between the vanes is very significant in the seven-vane configuration. In this case, the temperature between the vanes does not fall below 400 K, and is clearly higher at both the cold and the hot sides of the vanes as compared to the two-vane configuration. Note that the actual gas temperatures at the vane surfaces are about 20 K lower than the corresponding surface temperature due to the finite Knudsen number resulting in noticeable temperature jump at the surface. The imposition of the diffuse boundary condition at the walls results in fast decrease of temperature near the chamber walls parallel to the vanes, where it is about 310 K. As the flow streamlines show, the thermal creep dominates the bulk gas motion, as the gas generally moves from the cold side of the radiometer through the gaps to the hot side. The effect is also similar to the thermal transpiration phenomenon, although the latter one is observed at higher Knudsen numbers.

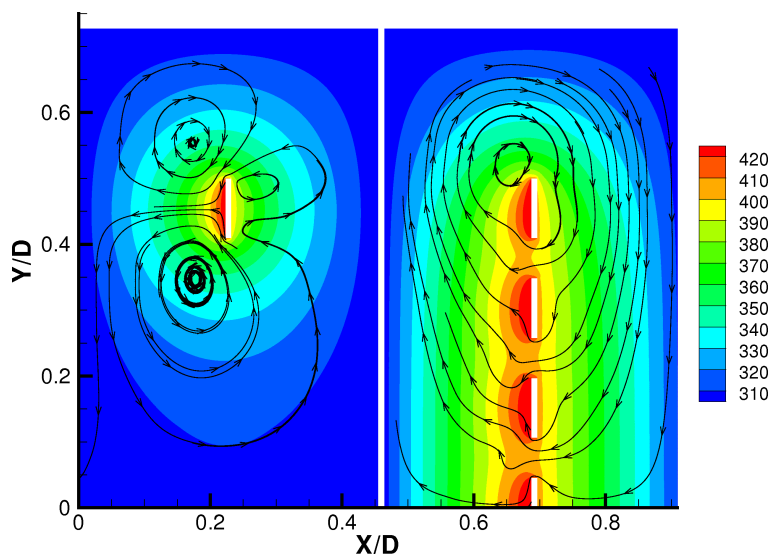


**Figure 1.** Temperature fields and streamlines for two-vane (left) and seven-vane (right) configurations in a small chamber.  $Kn = 0.05$ .

The above results were obtained at a Knudsen number where the radiometric force is near its maximum. The complete set of results obtained for different Knudsen numbers and number of vanes are given in Fig. 2. Since the main subject of this study is the force on the working sides of the vanes (called pressure force here), and not the shear force on the lateral sides of the vanes (which can be changed varying the thickness of the radiometer vanes), only the pressure force is presented. Note that in the range of pressures and geometries shown in Fig. 2, the shear force, which generally acts toward the reduction of the total radiometric force, is only a few percent of the pressure force, and thus is not important. Several conclusions may be drawn from the presented results. First, the general bell-shaped form of pressure dependence of the radiometric force observed for single vane radiometers,<sup>20</sup> is still observed for multi-vane configurations. Second, as the number of vanes increases and the separation between them decreases, the maximum shifts in the range of smaller Knudsen numbers (and thus higher pressures). For a two-vane configuration, the maximum is observed at  $Kn \sim 0.1$ , whereas for the nine vane configuration it occurs at  $Kn \sim 0.03$ . The reason for this appears to be that as the distance between vanes decreases, the thermal creep flow becomes more pronounced, that redistribute gas from cold to hot, and generally has larger impact at higher gas densities. Third, and most important, the radiometric force significantly increases as the separation between the vanes decreases.

The maximum pressure force as a function of the separation between the vanes is shown in Fig. 3. In

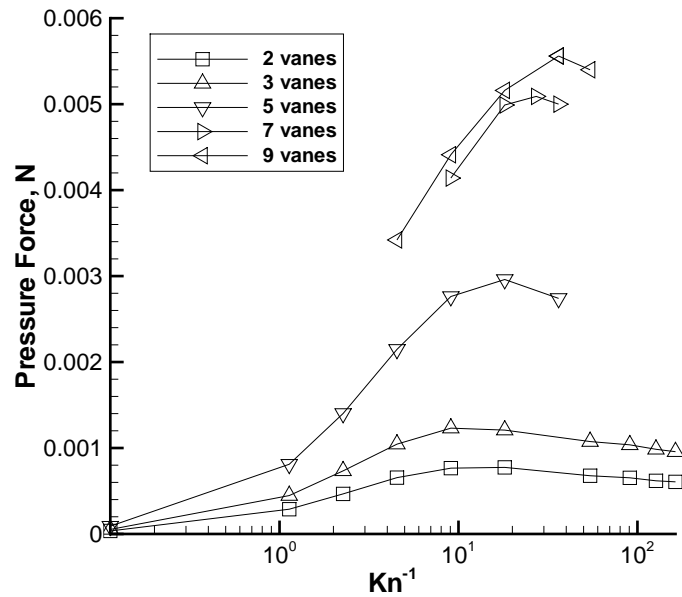
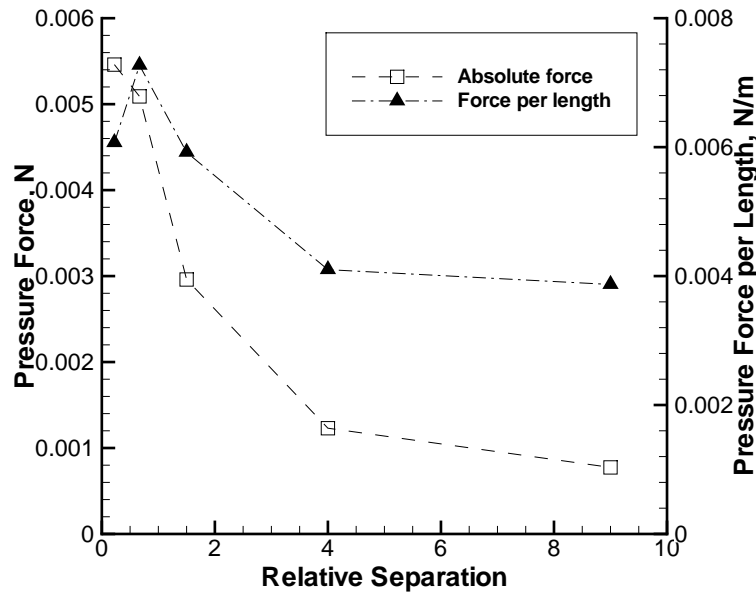


Figure 2. Dependence of pressure force on the vane separation as a function of gas density. Small chamber.

this figure, the X axis was normalized by the length of a single radiometer vane. It is clearly seen that the radiometric force is largest when the separation is about 0.25 of the vane size. Note however that further decrease of the separation is expected to reduce the force. In the limiting case of zero separation (one large vane) the radiometric force was found to be only about one third of its maximum. One important measure of the radiometer performance is the force produced per unit of its active length, i.e. in effect the force per mass ratio (for the two-vane configuration, the active length is  $0.18D$ , for three vane it is  $0.27D$ , etc.) The force per length ratio, also given in Fig. 3, illustrates the efficiency of the seven-vane configuration, where the height of the gaps between the vanes is close to the size of the vanes. Further decrease of the gap height starts to obstruct the thermal creep flow, thus resulting in the decrease of the radiometric force per vane. For larger gaps, the thermal creep loses its efficiency, and becomes virtually non-existent when the gap to vane height ratio approaches ten.

The pressure difference between the hot and the cold side of the radiometers, presented in Fig. 4, allows for a quantitative analysis of the impact of the interference between the vanes and the thermal creep flow. In this figure,  $X/D = 0$  represents the symmetry plane, and  $X/D = 0.5$  corresponds to the outer edge of



**Figure 3.** Maximum pressure force, absolute and per radiometer length, for different vane separations. Small chamber.

the radiometer. The results are shown for a Knudsen number of about 0.05 (gas pressure 1,000 Pa), where the radiometric force is near its maximum. Let us first consider the two-vane configuration. In this case, only one vane is shown, located between  $X/D = 0.41$  and  $X/D = 0.5$ . It is clearly seen that the pressure difference distributed over the vane, and thus radiometric force, increase near the edge, and has a minimum in the center. Such a behavior, caused by the combined effect of edge and area forces,<sup>10</sup> is typical for flat plate radiometers. The area force mentioned above is in effect a free molecular force<sup>21</sup> where the molecules colliding with the hot side of a radiometer leave with an increased velocity relative to those colliding with the cold side. The edge force first mentioned in Ref.<sup>22</sup> is an unbalanced force that exists near the edge of the heated side of the vane, where the heat flow in the gas is non-uniform.

Note that there is not visible difference between the left and right edges of the vane, which illustrates the negligible effect of the interference between two vanes. For the three-vane configuration (there is an additional vane in the middle as compared to the two-vane setup), the pressure difference at the outer vanes is slightly higher than for the two-vane case due to the stronger interference between the vanes. The force at the inner edge of the outer vane is a few percent higher than at the outer edge of that vane. For the

seven-vane case, the pressure difference at the outer edge is almost two times larger than for the smaller number of vanes. Note that the center vanes are about 20% more efficient than the outer ones. This is related to the more efficient gas transfer by the creep flow in that region, which may also be stimulated by the proximity of the chamber walls. Further increase in the number of vanes results in decrease of the pressure difference on the vanes, which is primarily related to the significant reduction of the edge forces (they are about two t

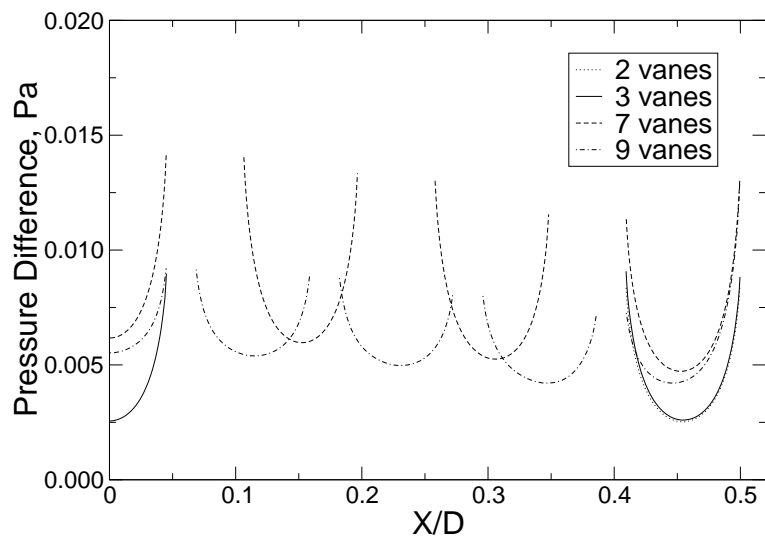


Figure 4. Pressure difference between the hot and the cold sides for different vane separations. Small chamber.

#### IV. Maximum radiometric force per area

The results presented in the previous section have shown that the radiometric device is most efficient when the size of the gaps that separate the vanes is about the size of the vanes. In this case, the radiometric force is maximum at a Knudsen number of about 0.05. One can assume that further increase in radiometric force may be achieved by reducing the size of the radiometer vanes while keeping the same gap to vane height ratio (thus increasing the number of vanes). In this case, if the maximum force is observed at approximately the same Knudsen number of 0.05, the correspondingly larger gas pressure may result in larger total radiometric force. In order to analyze this hypothesis, the computations were conducted for 14 and 21 vane configurations, in addition the the 7 vane case considered above. In these three cases, the same gap-to-vane height ratio of 0.75 is maintained. The results are compared to the case of a single large

radiometer vane with the same area as the effective area of the multi-vane configurations.

Let us first compare the flow in a single vane and 21 vane configurations. Gas temperature fields and streamlines for these cases are presented in Fig. 5. In both cases, the initial gas pressure was 1,000 Pa, which corresponds to a Knudsen number of about 0.005 for the single vane and 0.15 for the multi-vane configuration. The Knudsen number is much larger in the latter case since it is based on the height of a small vane. Note that the large chamber scenario is shown here in order to illustrate the flow with smaller impact of the chamber walls as compared to Fig. 1. The temperature fields are relatively close, with the 21 vane flow behaving qualitatively similar to the single vane case. The gas temperature in the vicinity of the hot surface near the symmetry plane approaches 444 K for 21 vanes versus 442 K for a single vane. At the cold side, the temperatures are 404 K and 410 K, respectively. The gas temperatures further away from the surface are very close. Even though the temperature fields are similar for the two cases under consideration, the bulk gas motion is qualitatively different. In the single vane case, there are four vortices created, two at each side of the radiometer (only two are shown here as the computations use a symmetry plane at  $Y = 0$ ). Such a flow patten generally resembles the case of a very large chamber considered in.<sup>13</sup> For the multi-vane configuration, there is a circular motion in the direction from cold to hot sides of the vanes. The large vortex shown in the upper half of the chamber is driven by the thermal creep. It is interesting to note that the magnitude of the flow velocities is nearly the same for the two configurations, approaching approximately 0.5 m in front of the hot side of the radiometer.

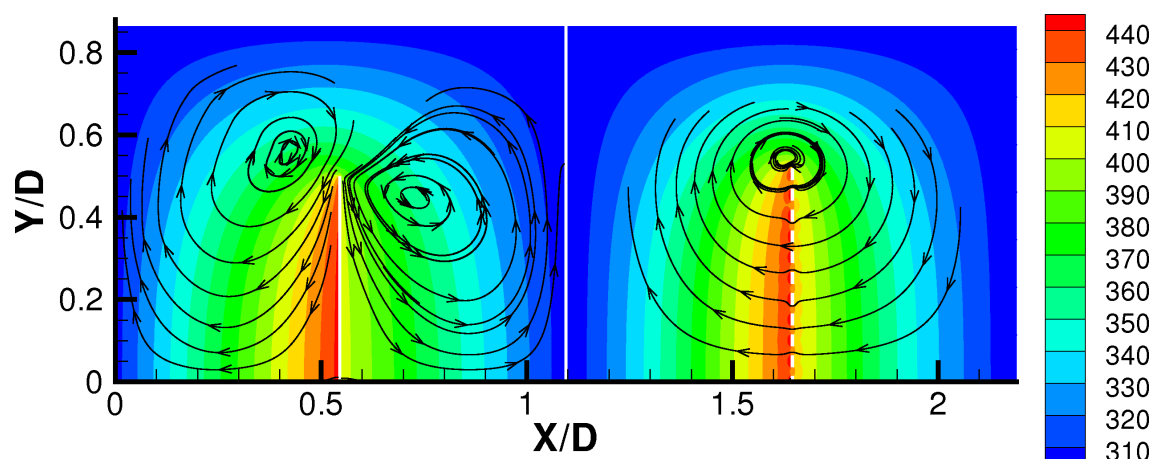


Figure 5. Temperature fields and streamlines for a single vane (left) and 21 vane (right) radiometers in a large chamber.

Let us now examine the impact of changing the gas pressure on the distributed radiometric force in the single and multi-vane geometries. The pressure difference between the hot and cold sides along the surface of a single vane is given in Fig. 6 for a Knudsen number decreasing from 0.8 to 0.005, which corresponds to the pressure range from 0.006 Pa to 1 Pa. For the largest considered Knudsen number, where the thermal creep is insignificant, and the edge force is virtually non-existent, the total radiometric force is driven by the area force only. As a result, the pressure difference is practically constant along the vane. The increase in gas pressure by a factor of ten ( $Kn = 0.08$ ) causes an approximately factor of four increase in the radiometric force. The reason for the increase being less than linear is molecular collisions between the hot molecules reflected on the vane surface and the cold incoming molecules, which effectively reduce the momentum transferred to the vane. Also note that for this Knudsen number there is a visible contribution of the edge force. This contribution becomes even more pronounced as the Knudsen number decreases to 0.02. Further decrease in  $Kn$  to 0.005 causes a noticeable reduction in the pressure difference in the central region, since the molecular collisions degrade the area force generation. The force at the edge is much larger than for all previous cases. However, since the edge force is generally proportional to the mean free path, the region where it is significant is relatively small, and does not compensate for the decrease in the central region. The pressure difference for  $Kn = 0.005$  is somewhat larger at  $X/D = 0$  (symmetry plane) than at  $X/D \approx 0.35$  due to the proximity of the chamber walls.

The impact of the area and edge forces is also clearly seen in Fig. 7 where the pressure difference is presented along a seven-vane radiometer at four different pressures. The pressure difference along each vane in the multi-vane configuration is qualitatively similar to that of a single vane configuration with a similar Knudsen number. For a Knudsen number of 0.22, the force at the vane edges is about 30% larger than that in the middle of the vanes. The difference between the forces produced by central and outer vanes is relatively small in this case (less than 10%). The difference increases with gas pressure, and reaches about 25% for  $Kn = 0.0276$ . Similar to the single vane configuration, the increase in pressure also increases the forces on the edges of the vanes and reduces forces at their centers. The maximum total force is observed at  $Kn = 0.0368$ .

The radiometric forces for different Knudsen numbers and numbers of vanes are presented in Fig. 8. In this figure, dashed lines represent the forces generated by the pressure difference between the hot and cold

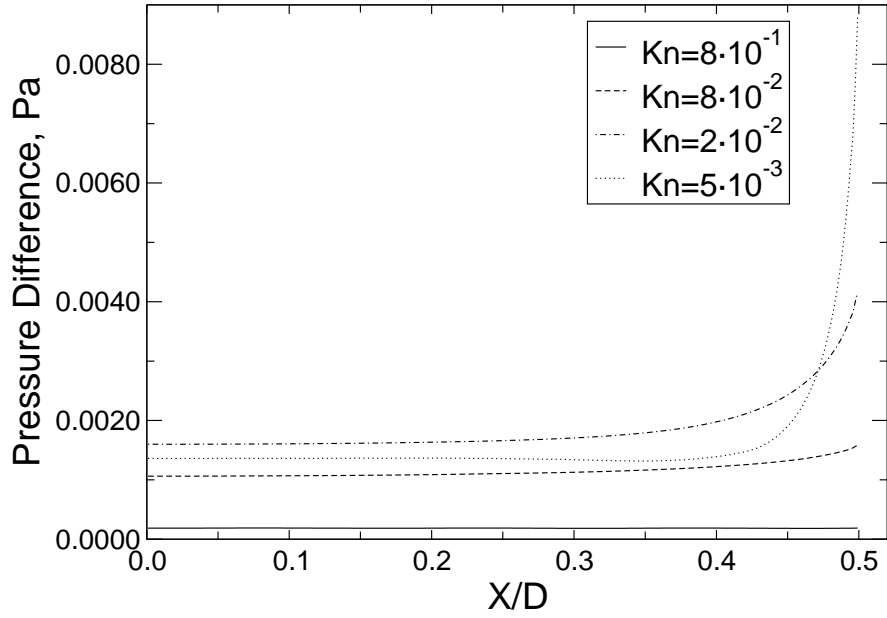


Figure 6. Pressure difference between the hot and the cold sides in a single vane radiometer. Small chamber.

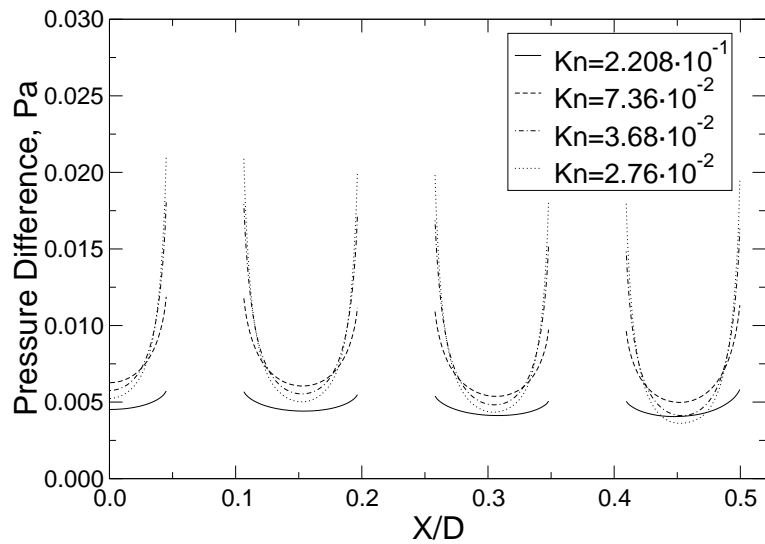
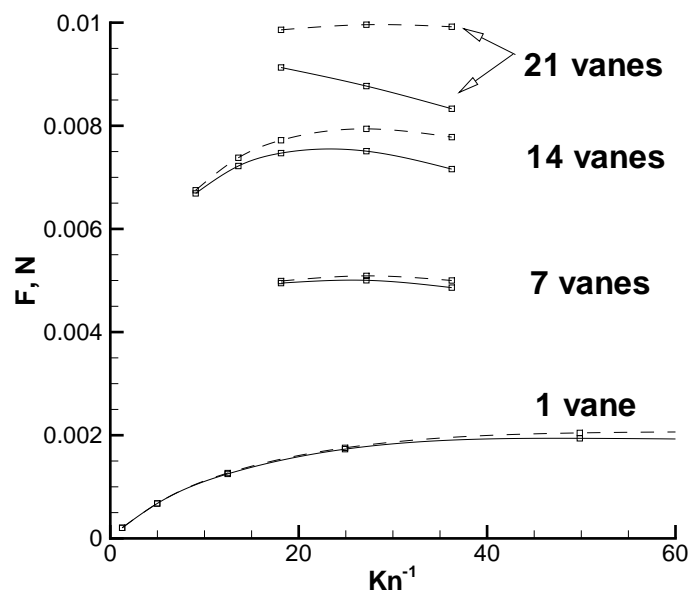


Figure 7. Pressure difference between the hot and the cold sides in a seven-vane radiometer. Small chamber.

sides of the vanes (pressure force), and the solid lines show the total force that includes the contribution of both the pressure force and the shear force on the lateral sides of the vanes. It is seen that the reduction in the vane size results in the increase of the force, both pressure and total, for all Knudsen numbers under consideration. The maximum pressure force slightly shifts to the left as the number of vane increases from one to seven. For a single vane, the pressure force was maximum at a Knudsen number of about 0.02, whereas for 7 vanes its maximum is observed at  $Kn \approx 0.03$ . Further increase in the number of vanes does not shift the pressure force maximum. The total force maximum shifts somewhat to the left for larger number of vanes, as the shear force begins to contribute. As expected, the contribution of the shear force increases with the inverse Knudsen number and the number of vanes. The smaller Knudsen number, and thus higher gas pressure, causes stronger cold to hot gas flow. The larger number of vanes is associated with larger shear forces both due to the increase in the lateral area and the increase in gas pressure at a fixed Knudsen number.



**Figure 8. Pressure and total forces for different number of vanes in the radiometer as a function of gas density. Small Chamber.**

The results for two chambers and different numbers of vanes are summarized in Fig. 9 where the maximum pressure and total forces are presented. Several conclusions may be drawn from these results. Most

importantly, the performance of a radiometric device may be significantly improved when holes are made in the radiometer vane, so that the radiometer consists of a number of smaller vanes. Extrapolating the results to larger number of vanes, it is expected that the pressure force may be increased by at least a factor of six, and the force to mass ratio by a factor of ten, as compared to a single vane geometry that uses the same effective area. Such an improvement in performance does not seem to be affected by the chamber size. While the increase in the chamber size generally reduces the radiometric force (this fact was previously observed in,<sup>13</sup> one can still expect about an order of magnitude increase in performance. The shear force on the lateral sides of the vanes may be a significant obstacle in achieving the optimum force. The thickness of radiometers vanes should therefore be reduced as much as possible in order to prevent the force degradation. Note that all results presented above are two-dimensional, and an additional resource of the force to mass increase could be cutting holes in the third dimension, perpendicular to the modeling plane (see Fig. 5). While the theoretical maximum in the performance increase is two orders of magnitude as compared to the single vane configuration, the actual force on such a three-dimensional geometry is difficult to estimate without detailed computations or experiments.

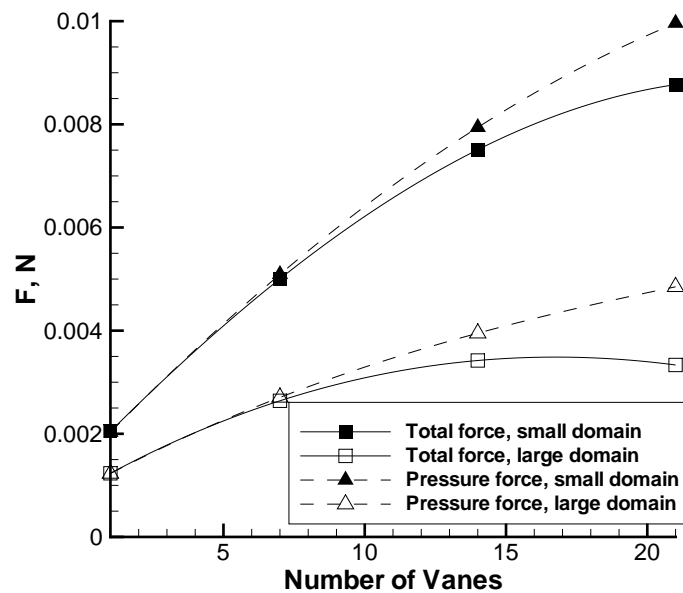


Figure 9. Maximum pressure and total forces versus the number of vanes in the radiometer for two chamber sizes.

## V. Conclusions

Numerical simulations were conducted at the kinetic level to study the possibility of increasing the efficiency of radiometric devices through etching holes in their working surfaces. The ES model kinetic equation was solved for a two-dimensional setup with a thin flat radiometer consisting of a single or multiple vanes of different height. In all cases, the total height of the radiometer was kept at 1.1 mm, and the minimum size of a single vane was about 27  $\mu\text{m}$ . A wide range of pressures was considered, with the corresponding Knudsen numbers varying from 10 to 0.005 based on the vane size. Two different chamber sizes were examined in order to illustrate the effect of the proximity of chamber walls.

It was found that a radiometer that consists of small vanes is much more efficient in terms of force production per radiometer mass than a solid plate radiometer that takes up the same effective area. In two-dimensional configuration, the increase is ten-fold. This increase was not visibly impacted by the chamber size. Further increase is expected for a three-dimensional configuration of a radiometer comprised of thin square vanes that are lined up on a plane and separated in longitudinal and transverse directions. The main phenomenon that causes such a large increase in radiometric force is thermal creep. There is also a combined effect of area and edge effects that influence the radiometric force at low and high pressure conditions, respectively.

Optimum separation between the radiometer vanes was observed when the size of the gaps between the vanes is comparable to the size of the vanes. The radiometric force per mass ratio approaches its maximum when the gap-to-vane height ratio is about 0.75. Increase in the number of vanes and proportional decrease in their size generally increases the radiometer efficiency, although using the vanes smaller than 10  $\mu\text{m}$  is not expected to provide any significant benefit. In this case, the interference between the vanes becomes an obstacle to the further increase in total force output. In all cases under consideration, the force maximum was observed at a Knudsen number of about 0.03; there is a relatively weak dependence of its location on the vane separation and number of vanes. The shear force on the lateral sides of the vanes was shown to be significant when the vane height-to-thickness ratio is less than 10; thinner radiometer vanes are therefore desirable for efficient device operation.

## VI. Acknowledgments

The authors are thankful to Drs. Ingrid Wysong and Dean Wadsworth for the interest that they expressed in this work, and for many fruitful discussions. The work was supported by the Air Force Office of Scientific Research.

## References

- <sup>1</sup>Johnson WA and Warne LK (1995) Electrophysics of micromechanical comb actuators. *J. Microelectromech. Sys.*, 4: 49-59
- <sup>2</sup>Chan EK and Dutton RW (2000) Electrostatic micromechanical actuator with extended range of travel. *J. Microelectromech. Sys.*, 9: 321-328
- <sup>3</sup>Kueppers H, Leuerer T, Schnakenberg U, Mokwa W, Hoffmann M, Schneller T, Boettger U, and Waser R (2002) *Sensors and Actuators*, 97-98: 680-684.
- <sup>4</sup>Roemer M, Kurzenknabe T, Oesterschulze E, and Nicoloso N (2002) Microactuators based on conducting polymers. *Anal. Bioanal. Chem.*, 373: 754-757.
- <sup>5</sup>Van De Pol FCM, Wonnink DGJ, Elwenspoek M, and Fluitman JHJ (1989) A thermo-pneumatic actuation principle for a microminiature pump and other micromechanical devices. *Sensors and Actuators*, 17: 139-143.
- <sup>6</sup>Muntz EP, Shiflett GR, Erwin DA (1992) Transient energy-release pressure-driven microdevices. *J. Microelectromech. Sys.*, 1: 155-163
- <sup>7</sup>Wadsworth DC and Muntz EP (1996) A computational study of radiometric phenomena for powering microactuators with unlimited displacements and large available forces. *J. Microelectromech. Sys.*, 5: 59-65
- <sup>8</sup>Passian A, Wig A, Meriaudeau F, Ferrell T, and Thundat T (2002) Knudsen forces on microcantilevers. *J. Appl. Phys.*, 92: 6326-6333
- <sup>9</sup>Heo JS and Hwang YK (2005) Heat transfer in a micro-actuator operated by radiometric phenomena. *J. Mech. Sci. and Tech.*, 19: 664-673.
- <sup>10</sup>Selden N, Ngalande C, Gimelshein S, Muntz EP, Alexeenko A, Ketsdever A (2009) Area and edge effects in radiometric forces. *Phys. Rev. E* 79:041201
- <sup>11</sup>Loeb LB (1961) *The kinetic theory of gases*, 3rd edition, Dover Publications.
- <sup>12</sup>Selden N, Gimelshein N, Gimelshein S, Ketsdever A (2009) Analysis of accommodation coefficients of noble gases on aluminum surface with an experimental/computational method. *Phys. Fluids* 21(7):073101
- <sup>13</sup>Selden N, Ngalande C, Gimelshein N, Gimelshein S, Ketsdever A (2009) Origins of radiometric forces on a circular vane with a temperature gradient. *J. Fluid Mech.* 634:419-431.

<sup>14</sup>Young M, Keith S, and Pancotti A (2009) An overview of advanced concepts for near space systems. AIAA paper 2009-4805. 45th Joint Propulsion Conference, Denver, CO.

<sup>15</sup>Bhatnagar PL, Gross EP, Krook M (1954) A model for collision processes in gases I: Small amplitude processes in charged and neutral one-component systems. Phys. Rev. 94:511-525

<sup>16</sup>Holway LH (1966) Numerical solutions for the BGK-model with velocity dependent collision frequency. Proc. IV Int. Symp. on Rarefied Gas Dynamics, New York Academic Press 193-215

<sup>17</sup>Mieussens L (2000) Discrete-velocity models and numerical schemes for the Boltzmann-BGK equation in plane and axisymmetric geometries. J. Comp. Phys. 162:429-466

<sup>18</sup>Wadsworth DC, Gimelshein NE, Gimelshein SF, Wysong IJ (2008) Assessment of Translational Anisotropy in Rarefied Flows Using Kinetic Approaches, Proc. XXVI Int. Symp. on Rarefied Gas Dynamics, Kyoto, Japan, 21-25 July 2008.

<sup>19</sup>Bird GA (1994) Molecular Gas Dynamics and the Direct Simulation of Gas Flows. Clarendon Press, Oxford.

<sup>20</sup>West GD (1920) On the forces acting on heated metal foil surfaces in rarefied gases. Proc. Physical Soc. London. 32:166-189

<sup>21</sup>Reynolds O (1876) On the forces caused by the communication of heat between a surface and a gas; and on a new photometer. Phil. Trans. R. Soc. 166:725-735

<sup>22</sup>Maxwell JC (1879) On stresses in rarified gases arising from inequalities of temperature. Phil. Trans. of Royal Soc. London. 170:231-256